A R C H I V E S O F M E T A L L U R G Y A N D M A T E R I A L S
Volume 60 2015 Issue 2
DOI: 10.1515/amm-2015-0225

M. RĘKAS*,#

ELECTROLYTES FOR INTERMEDIATE TEMPERATURE SOLID OXIDE FUEL CELLS

ELEKTROLITY DO ŚREDNIO-TEMPERATUROWYCH STAŁO-TLENKOWYCH OGNIW PALIWOWYCH

Solid electrolytes for construction of the intermediate-temperature solid oxide fuel cells, IT-SOFC, have been reviewed. Yttrium stabilized tetragonal zirconia polycrystals,YTZP, as a potential electrolyte of IT-SOFC have been highlighted. The experimental results involving structural, microstructural, electrical properties based on our own studies were presented. In order to study aluminum diffusion in YTZP, aluminum oxide was deposited on the surface of 3 mol.% yttria stabilized tetragonal zirconia polycrystals (3Y-TZP). The samples were annealed at temperatures from 1523 to 1773 K. Diffusion profiles of Al in the form of mean concentration vs. depth in B-type kinetic region were investigated by secondary ion mass spectroscopy (SIMS). Both the lattice (D_B) and grain boundary (D_{GB}) diffusion were determined.

Keywords: Intermediate temperature solid oxide fuel cells IT-SOFC, solid electrolytes, tetragonal zirconia, electrical properties, lattice and grain boundary diffusion

Dokonano przeglądu literaturowego elektrolitów stałych do konstrukcji średnio-temperaturowych stało-tlenkowych ogniw paliwowych. Tetragonalna polikrystaliczna cyrkonia stabilizowana itrem (YTZP) była przedmiotem badań. Wyniki eksperymentalne obejmowały badania strukturalne, mikrostrukturalne oraz właściwości elektryczne. Na powierzchni spieku 3YTZP nanoszono tlenek glinu, w celu określenia dyfuzji glinu. Próbki wygrzewano w zakresie temperatur 1523-1773 K. Profile dyfuzji określano, jako średnia koncentracja Al w funkcji głębokości w zakresie kinetycznym B-typu, stosując spektroskopię masową jonów wtórnych (SIMS). Wyznaczono współczynniki dyfuzji Al: w sieci (D_B) oraz po granicach ziaren (D_{GB}).

1. Introduction

Fuel cells efficiently convert directly chemical energy of the fuels into electricity (and heat) in a silent and environmentally friendly way without involving the process of combustion. Their efficiencies are not limited by the Carnot cycle of a heat engine. However, significant efforts are still necessary to develop commercially feasibly fuel cells, in particularly to increase their long-term stability and reduce costs of their construction and maintenance.

Several different types of fuel cells have been proposed, so far:

- Alkaline fuel cell, AFC
- Polymer electrolyte membrane fuel cell, PEMFC
- Phosphoric acid fuel cell, PAFC
- Molten carbonate fuel cell, MCFC
- Solid oxide fuel cell, SOFC

Table 1 [1-6] summarizes above mentioned types of fuel cells including: type of fuel, composition of the main components (anode, electrolyte (mobile ion), cathode, interconnect) and operating temperature. SOFCs attract great interest due to their high-energy conversion efficiency, fuel flexibility (H_2, CO, hydrocarbons). They are also environmentally friendly and allow for the possibility of recovering exhaust heat. Mainly hydrogen is used as a fuel in SOFC, but the high temperature (above 650°C) allows internal reforming of carbon-containing fuel at the anode.

The aim of this paper is to review solid electrolytes for use in intermediate temperature solid oxide fuel cells (IT-SOFC) with specific emphasis on the tetragonal zirconia electrolyte.

2. SOFC

SOFCs are the most promising fuel cell type in terms of their potential market competitiveness because SOFCs:

- are most efficient in converting fuel input to electricity output, are flexible in the choice of fuel (H_2, CO, natural gas, LPG, ammonia and even coal), any impurities of fuel do not play role;
  - technology is most suited to applications in the distributed electricity generation;
  - have a modular and solid state construction and do not have any moving parts, thereby are quiet enough to be installed indoors;
  - the high operating temperature produces high quality heat byproduct for use in combined cycle applications;
- do not contain noble metals;
  - do not have problems with electrolyte management;

* FACULTY OF MATERIALS SCIENCE AND CERAMICS, AGH UNIVERSITY OF SCIENCE AND TECHNOLOGY, AL. A. MICKIEWICZA 30, 30-059 KRAKÓW, POLAND
# Corresponding author: rekas@agh.edu.pl

TABLE 1

Fuel cell types and selected features

Features	TYPE OF FUEL CELL					
	PEMFC polymer electrolyte membrane fuel cell	**AFC alkaline fuel cell**	**PAFC phosphoric acid fuel cell**	**MCFC molten carbonate fuel cell**	**PCFC protonic ceramic fuel cell**	**SOFC Solid oxide fuel cell**
Electrolyte	Hydrated polymer (nafion, F- teflon)	Aqueous KOH	H_3PO_4	Molten carbonate in $LiAlO_2$	Acceptor doped cerate of Ba or Sr	Yttria-stabilized zirconia (8YSZ)
Mobile ion	$(H_2O)_nH^+$	OH^-	H^+	CO_3^{2-}	H^+	O^{2-}
Cathode	Pt or Pt/C	Li-NiO	Pt/C	Li-NiO	Perovskite oxides	$(La,Sr)MnO_3$
Anode	Pt or Pt/C	Ni	Pt/C	Ni-Cr	Ni	Ni-YSZ
Catalyst	Pt	Pt	Pt	-	-	-
Interconnect	C or metal	metal	graphite	steel or ceramic	steel or ceramic	steel or ceramic
Operating temperature [°C]	40-50	65-220	150-250	500-700	600-700	600-1000
Fuel	H_2 or CH_3OH	H_2	H_2	hydrocarbons, CO	H_2	H_2, hydro-carbons, CO
Efficiency [%]	40	40-50	40	45	45-50	45-60

- have extremely low emissions, in particularly any CO produced is converted to CO_2;
- have a long life expectancy (more than 40 000-80 000 hrs).

Fig. 1 [7] illustrates schematically the principle of SOFC operation.

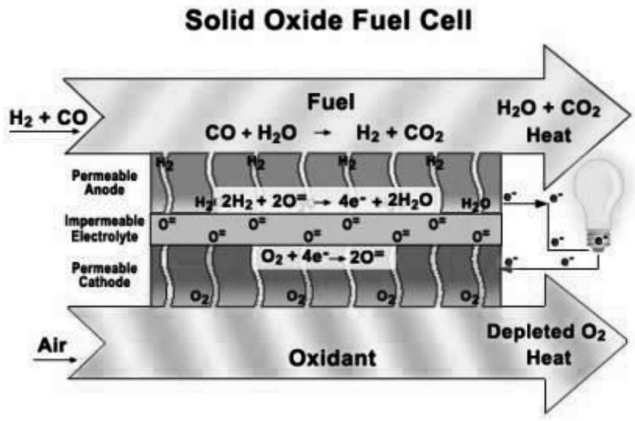

Fig. 1. Operating concept of a SOFC (from: http://www.seca.doe.gov)

3. IT-SOFC

SOFCs have long been limited by the necessity to operate at high temperatures (800-1000°C) causing prolonged start up times and materials constraints. This operating temperature makes them costly due to the necessity of a more exotic interconnect ($(La,Sr)CrO_3$) and housing components that can handle such temperatures. Also, at these temperatures electrode sintering, interfacial diffusion between the electrodes and the electrolyte and mechanical stress due to thermal incompatibilities are of great concern.

Decreasing the operating temperature is a main goal for the current R&D of SOFC. Reducing the operation temperature of SOFC below 750°C enables the use of a wide range of materials that allow cheaper fabrication, in particular metallic interconnects. Lower temperature operation can extend the lifetime of the cell stack reducing the corrosion rate and improving durability by slowing down sintering, and component inter-diffusion also enables more rapid start-up and shut down. The lower limit of the operating temperature is determined by internal reforming of hydrocarbons if they are used as fuel. This process proceeds above 600°C [8].Therefore, the goal of a lot of research efforts has been to reduce the operation temperature of the SOFC to the range 600-750°C.

4. Electrolytes for IT-SOFC

Solid electrolytes used in fabrication of fuel cells should meet numerous requirements such as:

- fast ionic transport;
- negligible electronic conductivity;
- thermodynamic stability over a wide range of oxygen partial pressures and operating temperatures;
- long-term stability;
- thermal expansion compatible with the electrodes and construction materials;
- suitable mechanical properties;
- negligible reactivity with electrode materials under operation conditions;
- lack of open porosity;
- low material, manufacturing and maintenance costs.

The most important property of a candidate electrolyte material is the ionic conductivity. Conductivity data of several candidates of IT-SOFC are presented in Fig. 2 [1, 6].

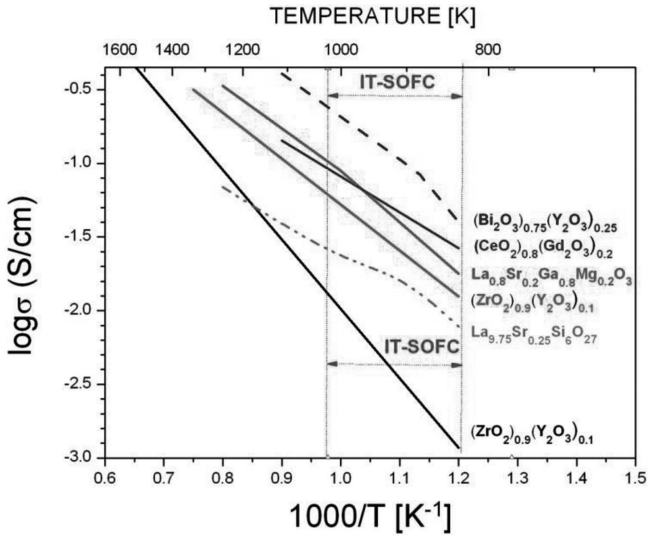

Fig. 2. Conductivity data of the most promising electrolytes- candidates to IT-SOFC

SOFCs with ZrO_2 containing 8 mol% Y_2O_3, 8YSZ, as an electrolyte are already in the advanced stage of development, and are therefore the first choice in the search for a suitable solid electrolyte for IT-SOFC. However the ionic conductivity of 8YSZ is relatively low at low temperatures. Some partial success has been obtained by fabricating the 8YSZ electrolyte film with a thickness of 10 μm or less in an anode supported SOFC configuration [9].

Yttria-stabilized δ-Bi_2O_3, which has a fluorite-type structure, shows the highest electrical conductivity [10, 11]. Unfortunately, this material has a number of drawbacks including thermodynamic instability in reducing atmosphere, volatilization of bismuth oxide at moderate temperatures, metastable structure below 870 K and low mechanical strength [10-12].

The most promising electrolyte material for IT-SOFC is CeO_2 doped with Gd_2O_3 [13]. Ceria CeO_2 has a fluorite structure and doping with Gd_2O_3 leads to the formation of oxygen vacancies, according to the reaction:

$$Gd_2O_3 \rightarrow 2Gd'_{Ce} + 3\,O^x_O O_O + V^{\bullet\bullet}_O \qquad (1)$$

Formed oxygen vacancies ($V^{\bullet\bullet}_O$) have a role in oxygen ionic conductivity. The ionic conductivity is a function of temperature and dopant concentration. The maximum ionic conductivity occurs at 10-20 mol % Gd_2O_3 [14]. Ceria based electrolytes suffer from the partial reduction of Ce^{4+} to Ce^{3+} under reducing conditions of the anode. It causes two negative effects: first, electronic (n-type) conductivity reduces the cell efficiency due to electronic leakage currents between the anode and cathode, and second, there is a volume expansion accompanying this process which can result in mechanical failure of the electrolyte [15]. In order to eliminate these negative effects Zhang et al [16] proposed to use a bi-layered electrolyte composed from Sm-doped CeO_2 with Sc-Doped ZrO_2 on the anode side.

Perovskite- type lanthanum gallates, $LaGaO_3$, possess high oxygen ionic conductivity (Fig. 2) and are thus promising electrolyte material for IT-SOFC. High oxygen ionic conductivity in $LaGaO_3$ can be achieved by partially substituting lanthanum and gallium ions with strontium and magnesium, respectively:

$$SrO + MgO \rightarrow Sr'_{La} + Mg'_{Ga} + 2\,O^x_O O_O + V^{\bullet\bullet}_O \qquad (2)$$

The maximum ionic conductivity of $La_{1-x}Sr_xGa_{1-y}O_{3-(x+y)/2}$, LSGM, is achieved at x=0.10-0.20 and y= 0.15-0.20. Further acceptor doping results in vacancy ordering, which leads to a decrease of conductivity (drop down of oxygen ion mobility) [17, 18].

High oxygen ion conductivity is observed also in apatite-type phases $A_{10-x}(MO_4)_6O_{2\pm\delta}$ where A corresponds to rare earth and alkaline earth elements, M=Si or Ge [19, 20]. The highest oxygen ionic conductivity is observed when apatite phases contain more than 26 oxygen atoms per unit formula, suggesting the interstitial oxygen migration mechanism. Decreasing oxygen concentration below the stoichiometric value leads to the vacancy mechanism and then a considerable drop in ionic conductivity is observed. In particular, an enhanced ionic transport was found in the material $La_{9.75}Sr_{0.25}Si_6O_{27}$ [21].

Based on the presented short review it can be concluded that possible choices for the IT-SOFC electrolytes are still limited, mainly to $LaGaO_3$-, CeO_2-, $La_{10-x}Si_6O_{26\pm\delta}$ – and ZrO_2 – based systems.

5. Tetragonal zirconia polycrystals TZP

According to the ZrO_2 –Y_2O_3 phase diagram at stabilizer concentration of 3-7 mol % Y_2O_3 both cubic and tetragonal phases can be retained in the microstructure. The microstructure of these ceramics consists of a cubic phase matrix in which the tetragonal phase is dispersed. This grade of Y_2O_3 solid solution is termed partially stabilized zirconia, PSZ. If a significant volume fraction of metastable tetragonal phase is present, these tetragonal precipitates give the ceramic good mechanical properties (strength and toughness) through a process known as transformation toughening [22].

ZrO_2 containing 1 to 3 mol % Y_2O_3 with a submicron grain structure (below critical grain size ca. 0.3 μm [23]) is named tetragonal zirconia polycrystal, Y-TZP. Due to its very high mechanical strength (>1GPa) and fracture toughness (>4-6 MPa.m$^{1/2}$) it is named ceramic steel [24]. At moderate temperatures below 700°C the grain interior of Y-TZP shows higher electrical conductivity (σ_b) than that of fully (YSZ) or partially stabilized (PSZ) zirconia [25, 26]. However, the total conductivity of Y-TZP is lower due to the high contribution of grain boundary resistivity, known as the blocking effect [27, 28]. Generally, there are two causes of the blocking effect.

The first cause is related to the presence of impurities, mainly silica, that are segregated on grain boundaries. Silicon can form a glassy layer that surrounds the zirconia grains. There are some controversies regarding the nature of this layer. Some authors claim that the formation of a continuous glassy layer takes place and subsequently oxygen ion transport across grain boundaries must proceed through this isolating layer [29, 30]. Other authors assert only partial wetting of grain boundaries by the silica phase with some direct grain-to-grain contact [31-33]. If this explanation is true, oxygen ion conduction takes place through direct contact between grains [34].

The second explanation of the blocking effect is the presence of electrical potential at grain boundaries, which results in barrier (Schottky barrier) to ion transport. According to Guo and Zhang [35] the grain boundary region is depleted of oxygen vacancies, and this is the reason for the blocking phenomenon in grain-to-grain contact [36].

6. Modification properties of TZP

Many efforts have been made to reduce the blocking effect in Y-TZP. It was found that the alumina added to the zirconia material acts as the silicon scavenger [37-39]. The added alumina reacts with silica, forming a stable mullite:

$$3Al_2O_3 + 2SiO_2 \rightarrow Al_6Si_2O_{13} \quad (3)$$

According to Butler and Drennan's [37] thermodynamic calculations reaction (3) is possible when the activity of silica is at least 0.03 at 1600°C. On the other hand, the reaction between zirconia and silica yields the unstable silicate $ZrSiO_4$, which dissociates above 1540°C. However, this compound is not stable in the presence of alumina:

$$2ZrSiO_4 + 3Al_2O_3 \rightarrow Al_6Si_2O_{13} + 2ZrO_2 \quad (4)$$

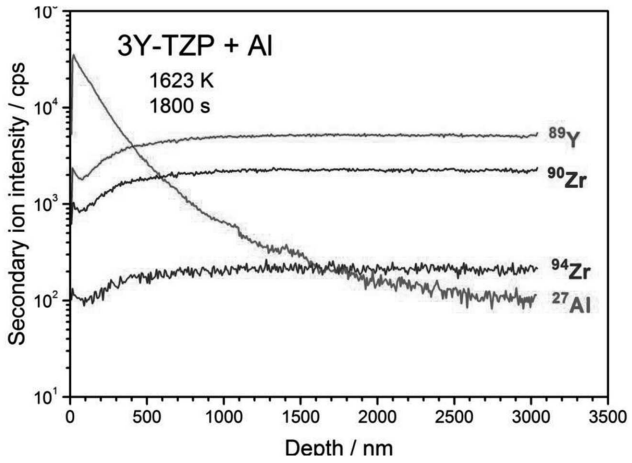

Fig. 3. Depth profiles of $^{27}Al^+$, $^{89}Y^+$, $^{90}Zr^+$ and $^{94}Zr^+$ isotopes obtaining after annealing at 1350°C for 0.5 h on terms of counts per second versus distance from the surface

The Gibbs free enthalpy of reaction (3) is negative above 920°C. The alumina/mullite system act as a buffer for silica, absorbing SiO_2 from any sources where it is present and exhibits higher activity than 0.03 [37]. Consequently, alumina acts as a silica scavenger. The addition of Al_2O_3 can influence both bulk and grain boundary conductivity of 3Y-TZP. The changes of interior grain conductivity may results from the solubility of alumina added to the zirconia lattice. According to Takeli [40], solubility limit of alumina in 8YSZ is about 0.3 wt %. Both solubility and scavenger effect of alumina is governed by high temperature diffusion of Al in the polycrystalline Y-TZP. Diffusion of aluminum in 3Y-TZP was studied by means of the secondary ion mass spectroscopy (SIMS) [41]. Fig. 3 illustrates distribution profile of Zr, Y and Al at 1623K after 0.5 h of the diffusion process. Using the theoretical equations proposed by Whipple [42] both lattice Al diffusion (D_B) and grain boundary Al diffusion (D_{GB}) coefficients were determined. Fig. 4 illustrates D_B and D_{GB} in the Arrhenius coordinate plots. The grain boundary Al diffusion coefficient assumes higher values than that of lattice coefficient.

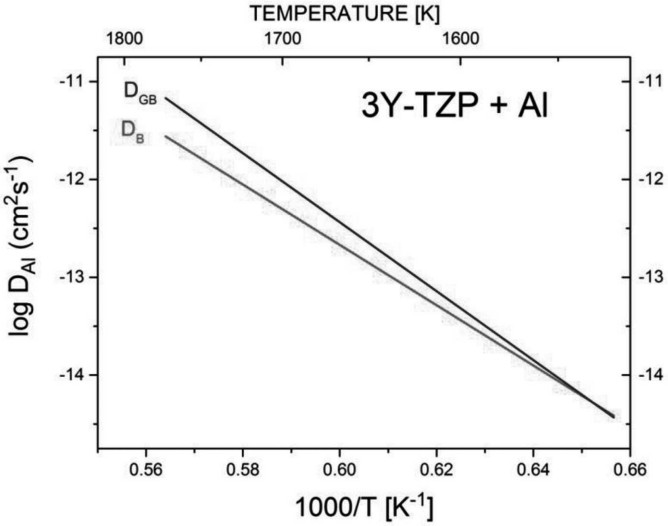

Fig. 4. Arrhenius plot of grain boundary diffusion coefficient (D_{GB}) and lattice diffusion coefficient (D_B) of Al in 3Y-TZP

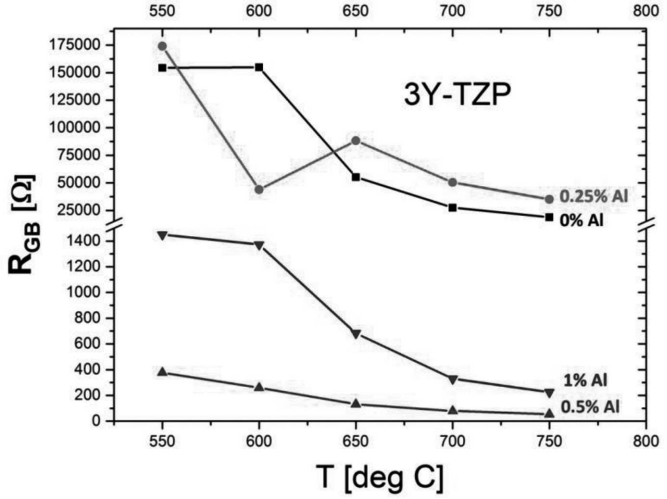

Fig. 5. Effect of aluminum content on grain boundary electrical resistivity

The effects of adding various amounts of aluminum oxide on the electrical properties of 3Y-TZP were studied by impedance spectroscopy [43]. Fig. 5 illustrates grain boundary resistivity versus temperature for various concentration of added alumina. The sample containing 0.5 mol% of alumina exhibits the lowest grain boundary resistivity. The effect of added alumina on grain interior resistivity is illustrated by Fig. 6. Again, the sample containing 0.5 mol% alumina exhibits the lowest grain interior resistivity. This sample (3Y-TZP+ 0.5 mol% Al_2O_3) has the lowest activation energy of the grain boundary conductivity (Fig. 7). It means that this material shows the smallest changes in grain boundary conductivity with temperature. Gadolinium oxide, Gd_2O_3, can also be used

as a modifier for Y-TZP grain boundary electrical properties. The results are described in [44].

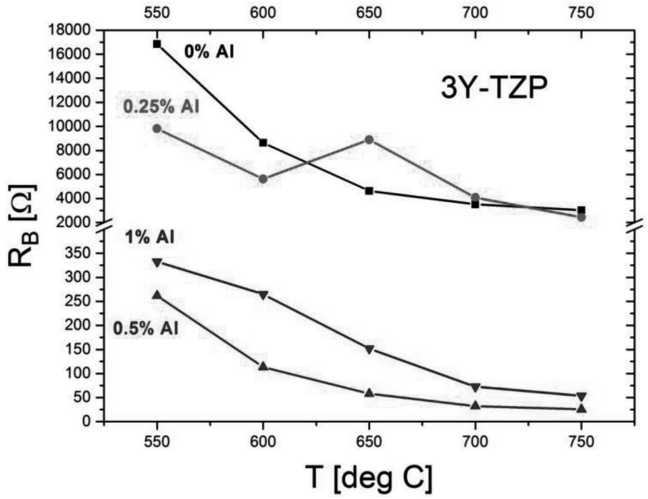

Fig. 6. Effect of aluminum content on grain electrical resistivity

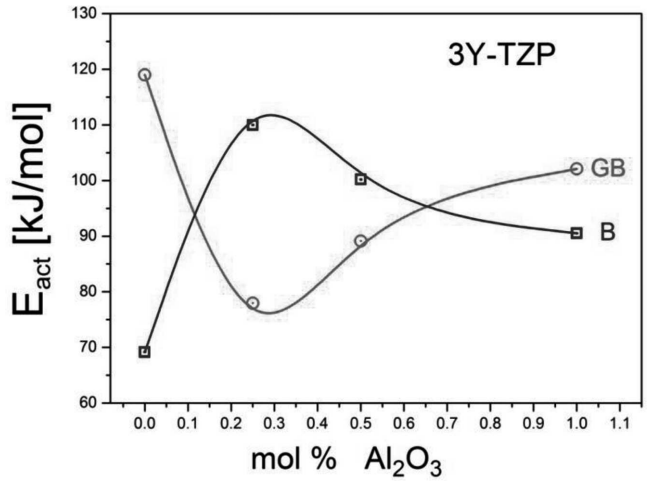

Fig. 7. Activation energy of the grains' electrical conductivity (B) and of the grain boundary conductivity (GB) versus alumina content

7. Conclusions

The most promising solid electrolytes for fabrication of intermediate temperature solid oxide fuel cells (IT-SOFC) were reviewed. Yttrium stabilized tetragonal zirconia polycrystals,YTZP, as a potential electrolyte of IT-SOFC has been highlighted. It was found, that modification by adding aluminum oxide to YTZP leads to preferable changes of electrical properties this material as solid electrolyte of IT-SOFC.

Acknowledgements

This work was supported by the Polish National Center of the Science (NCN) under Grant OPUS No. DEC -2012/05/B/ST8/02723.

REFERENCES

[1] O. Yamamoto, Electrochimica Acta **45**, 2423 (2000).
[2] S.P.S. Badwal, F.T. Ciacchi, Ionics **6**, 1 (2000).
[3] S. M. Haile, Acta Mater. **51**, 5981 (2003).
[4] V.V. Kharton, F.M.B. Marques, A. Atkinson, Solid State Ionics **174**, 135 (2004).
[5] D.J.L. Brett, A. Atkinson, N.P. Brandon, S.J. Skinner, Chem. Soc. Rev. **37**, 1568 (2008).
[6] E.V. Tsipis, V.V. Kharton, J. Solid State Electr. **12**, 1039 (2008).
[7] http://www.seca.doe.gov.
[8] A.I. Dicks, J. Power Sources **71**, 11 (1998).
[9] T. Van Gestel, F. Han, D. Sebold, Microsyst. Technol. **17**, 233 (2011).
[10] T. Takahashi, T. Esaka, H. Iwahara, J. Appl. Electrochem. **7**, 303 (1977).
[11] J.B. Goodenough, J.E. Ruiz-Dias, Y.S. Zen, Solid State Ionics **44**, 21 (1990).
[12] S. Boypati, E.D. Waschman, N. Jiang, Solid State Ionics **140**, 149 (2001).
[13] B.C.H. Steele, J. Mater. Sci. **36**, 1053 (2001).
[14] H. Yahiro, K. Eguchi, H. Arai, Solid State Ionics **36**, 71 (1989).
[15] M. Mogensen, N.M. Sammes, G.A. Tompsett, Solid State Ionics **129**, 63 (2000).
[16] X. Zhang, M. Robertson, C. Deces-Petit, Y. Xie, R. Hui, W. Qu, O. Kesler, R. Maric, D. Ghosh, J. Power Sources **175**, 800 (2008).
[17] T. Ishihara, H. Matsuda, Y. Takita, J. Am. Chem. Soc. **116**, 2801 (1994).
[18] M. Feng, J.B. Goodenough, Eur. J. Solid State Inorg. Chem. **31**, 663 (1994).
[19] S. Nakayama, M. Sakamoto, J. Eur. Ceram. Soc. **18**, 1413 (1998).
[20] A.L. Shaula, V.V. Kharton, F.M.B. Marques, J. Solid State Chem. **178**, 2050 (2005).
[21] H. Arikawa, H. Nishiguchi, T. Ishihara, Y. Takita, Solid State Ionics **136-137**, 31 (2000).
[22] K. Kobayashi, H. Kuwajima, T. Masaki, Solid State Ionics **3/4**, 489 (1981).
[23] M. Watanabe, S. Iio, I. Fukuhara, Advances in Ceramics, v. 12 Science and Technology of Zirconia II N. Claussen, M. Ruhle, A.H. Heuer, Eds, The American Ceramic Society, Inc. Columbus, Ohio p 391 (1984).
[24] R.C. Garvie, R.H. Hanning, R.T. Pascoe, Nature **258**, 703 (1975).
[25] W. Weppner, Adv. Ceram. **24**, 837 (1988).
[26] S.P.S. Badwal, J. Drennan, J. Mater. Sci. **24**, 8 (1989).
[27] N. Bonanos, R.K. Slotwinski, B.C.H. Steele, J. Mater. Sci. Lett. **3**, 245 (1984).
[28] D. Meyer, U. Eisele, R. Satet, J. Rödel, Scripta Mater. **58**, 215 (2008).
[29] M. Ruhle, N. Claussen, A.H. Heuer, Sci. Technol. Zirconia II, Adv. Ceram. **12**, 352 (1984).
[30] J. Tanaka, J.F. Baumard, P. Abelard, J. Am. Ceram. Soc. **70**, 637 (1987).
[31] A.E. Hughes, S.P.S. Badwal, Mater. Forum **15**, 26 (1999).
[32] T. Stoto, M. Neuer, C. Carry, J. Am. Ceram. Soc. **74**, 2615 (1991).
[33] T. Masaki, K. Sinjo, Ceram. Int. **13**, 109 (1987).
[34] S.P.S. Badwal, Solid State Ionics **76**, 67 (1995).
[35] X. Guo, Z. Zhang, Acta Mater. **51**, 2539 (2003).
[36] A.P. Santos, R.Z. Domingues, M. Kleitz, J. Eur. Ceram. Soc. **18**, 1571 (1998).
[37] E.P. Butler, J. Drennan (1982), J. Am. Ceram. Soc. **65**, 474 (1982).
[38] A.J. FeIghery, I.T.S. Irvine, Solid State Ionics **121**, 209 (1999).
[39] M.C. Martin, M.L. Mecartney, Solid State Ionics **161**, 67 (2003).

[40] S. Takeli, Mater. Design **28**, 713 (2007).
[41] K. Kowalski, K. Obal, Z. Pedzich, K. Schneider, M. Rekas, J. Am. Ceram. Soc. **97**, 3122 (2014).
[42] R.T.P. Whipple, Philos. Mag. **45**, 1225 (1954).
[43] K. Obal, Z Pedzich, T. Brylewski, M. Rekas, Int. J. Electrochem. Sc. **7**, 6831 (2012).
[44] J. Cyran, J. Wyrwa, E. Drozdz, M. Dziubaniuk, M. Rekas, this issue (2014).

Received: 20 February 2014.